MASARYKOVA UNIVERZITA
PŘÍRODOVĚDECKÁ FAKULTA
ÚSTAV TEORETICKÉ FYZIKY A ASTROFYZIKY

Bakalářská práce

BRNO 2022 MARTIN MAX

MASARYKOVA
UNIVERZITA
PŘÍRODOVĚDECKÁ FAKULTA
ÚSTAV TEORETICKÉ FYZIKY A ASTROFYZIKY

Modulace světelných křivek hvězd typu RR Lyrae v přehlídkových projektech

Bakalářská práce

Martin Max

Vedoucí práce: Mgr. Marek Skarka, Ph.D. **Brno 2022**

Bibliografický záznam

Autor:	Martin Max Přírodovědecká fakulta, Masarykova univerzita Ústav teoretické fyziky a astrofyziky
Název práce:	Modulace světelných křivek hvězd typu RR Lyrae v přehlídkových projektech
Studijní program:	Fyzika
Studijní obor:	Astrofyzika
Vedoucí práce:	Mgr. Marek Skarka, Ph.D.
Akademický rok:	2021/2022
Počet stran:	ix + 33
Klíčová slova:	Metody: analýza dat; hvězdy: horizontální větev; hvězdy: proměnné: RR Lyrae; přehlídky; techniky: fotometrie

Bibliographic Entry

Author:	Martin Max Faculty of Science, Masaryk University Department of Theoretical Physics and Astrophysics
Title of Thesis:	Modulation of the light curves of RR Lyrae type stars in the sky survey data
Degree Programme:	Physics
Field of Study:	Astrophysics
Supervisor:	Mgr. Marek Skarka, Ph.D.
Academic Year:	2021/2022
Number of Pages:	ix + 33
Keywords:	Methods: data analysis; stars: horizontal branch; stars: variables: RR Lyrae; surveys; techniques: photometric

Abstrakt

V této bakalářské práci prezentujeme výsledky analýzy frekvenčních spekter více než 500 datových sad pro 142 hvězd z několika různých přehlídek oblohy (ASAS-SN, SuperWASP, CSS, NSVS a QES). Při předzpracování dat jme použili program `Period04` a upřesnili tím hodnoty pulzačních period všech hvězd v našem vzorku. Pro hledání Blažkova jevu jsme použili interaktivní `Python` skript `BLSearch`. Identifikovali jsme 86 Blažkovych hvězd, z nichž jsme potvrdili, že 61 hvězd má Blažkovy periody blízké těm, které byly nalezeny na základě změn period. Zbývajících 25 hvězd vyžaduje další ověrení period. Přehlídka ASAS-SN se jeví jako nejvhodnejší pro hledáni Blažkova jevu, jelikož většina datových sad s identifikovaným Blažkovym jevem pochází z této přehlídky.

Abstrakt

V tejto bakalárskej práci prezentujeme výsledky analýzy frekvenčných spektier viac ako 500 dátových sád prislúchajúcich 142 hviezdam z niekoľkých rôznych prehliadok oblohy (ASAS-SN, SuperWASP, CSS, NSVS a QES). Pri predspracovaní dát sme použili program `Period04` a upresnili tým hodnoty pulzačných periód všetkých hviezd v našej vzorke. Pre hľadanie Blažkovho javu sme použili interaktívny `Python` skript `BLSearch`. Identifikovali sme 86 Blažkových hviezd, z ktorých sme potvrdili, že 61 hviezd má Blažkove periódy blízke tým, ktoré boli nájdené na základe zmien periód. Zvyšných 25 hviezd si vyžaduje ďalšie overenie periód. Prehliadka ASAS-SN sa javí ako najvhodnejšia pre hľadanie Blažkovho javu, keďže väčšina dátových sád s identifikovaným Blažkovým javom pochádza z tejto prehliadky.

Abstract

We present results of the frequency spectra analysis of more than 500 datasets for 142 RR Lyrae stars from multiple different sky surveys (ASAS-SN, SuperWASP, CSS, NSVS and QES). In the pre-processing of data for further analysis, we used `Period04` and improved pulsation periods of all of the stars from our sample. For searching for the Blazhko effect we used interactive `Python` script `BLSearch`. The number of Blazhko stars we identified is 86, out of which we confirmed 61 stars to have Blazhko periods close to those found on the basis of the period changes. Blazhko periods of remaining 25 stars need further verification. The ASAS-SN survey appears to be the most suitable for searching for the Blazhko effect, since majority of datasets with identified Blazhko effect comes from this survey.

MASARYKOVA UNIVERZITA
PŘÍRODOVĚDECKÁ FAKULTA
KOTLÁŘSKÁ 2, 611 37 BRNO
IČ: 00216224
DIČ: CZ00216224

ZADÁNÍ BAKALÁŘSKÉ PRÁCE

Akademický rok: 2020/2021

Ústav:	Přírodovědecká fakulta
Student:	Martin Max
Program:	Fyzika
Obor:	Astrofyzika

Ředitel *ústavu* PřF MU Vám ve smyslu Studijního a zkušebního řádu MU určuje bakalářskou práci s názvem:

Název práce:	Modulace světelných křivek hvězd typu RR Lyrae v přehlídkových projektech
Název práce anglicky:	Modulation of the light curves of RR Lyrae type stars in the sky survey data
Jazyk závěrečné práce:	angličtina

Oficiální zadání:
Modulace světelných křivek proměnných hvězd typu RR Lyrae je stále jednou z nevyřešených záhad. Student se v práci zaměří na potvrzení modulace a odhad její periody u hvězd galaktického pole, kde byl tento, tzv. Blažkův, jev odhalen na základě předchozí vizuální kontroly. Využije k tomu dat z přehlídkových projektů a provede srovnání vlastností nově objevených hvězd s vlastnostmi již známých modulovaných hvězd.

Vedoucí práce:	Mgr. Marek Skarka, Ph.D.
Datum zadání práce:	27. 11. 2020
V Brně dne:	11. 2. 2021

Zadání bylo schváleno prostřednictvím IS MU.

Martin Max, 21. 1. 2021
Mgr. Marek Skarka, Ph.D., 26. 1. 2021
Mgr. Michael Krbek, Ph.D., 1. 2. 2021

Poďakovanie

Na tomto mieste by som chcel poďakovať svojmu vedúcemu doktorovi Marekovi Skarkovi za trpezlivosť, ochotu a cenné rady pri spracovaní záverečnej práce. Zároveň by som chcel poďakovať svojim priateľom a rodine za pomoc a podporu počas celého štúdia.

Prehlásenie

Prehlasujem, že som svoju bakalársku prácu vypracoval samostatne pod vedením svojho vedúceho práce s využitím informačných zdrojov, ktoré sú v práci citované.

Brno 22. mája 2022 . . . . . .

Martin Max

Contents

Introduction

RR Lyrae stars represent one of the most important variable stars group. They belong to ”standard candles” in the cosmic distance ladder and they are mostly used for measuring distances to nearby objects within the Galaxy and the Local Group of galaxies. They are also great for the study of population II stars considering that they are old and evolved stars. They are easily distinguishable from other types of variable stars due to their specific light curves with relatively high amplitudes. All these attributes combined with relatively large occurrence makes them very efficient tool, not only for distance determination, but also for testing evolutionary and pulsation models, mapping the distribution and kinematics of population II stars or even tracing metallicity of evolved stars.

Over the last decades of intense space research with help of the modern technologies, many fields of astrophysics experienced great development. And stellar astrophysics with RR Lyrae research being no exception to that. Even though, there are still some unsurpassed barriers which are waiting to be resolved. The most significant of them is more than hundred years old mystery of the Blazhko effect (Blažko, 1907). The Blazhko effect is a quasiperiodic modulation of the pulsation amplitude and phase, which causes long term changes in the light curve shape of up to 50% RR Lyrae stars (Jurcsik et al., 2009). Modulation of the light curve is common effect amongst other pulsating variables such as δ Sct stars but the physics behind it might have different cause than in RR Lyraes.

RR Lyrae type stars

1.1 History of research

In the last decades of 19th century, observations of globular clusters revealed a large number of new variable stars (Pickering & Bailey, 1895). Most of them were showing similar periods and light curves. Bailey & Leland (1899) named them *Cluster variables* because of the location where they were found. First "cluster variable" outside the globular cluster (U Leporis) was discovered by Kapteyn (1890) and few years later the prototype star, RR Lyrae, was discovered by Fleming (1899) in the Lyra constellation. It became the eponym for this class of the variable stars. The light curves of the RR Lyrae stars were similar to the classical cepheids, but the periods of light variations was shorter, hence they called them *short-period cepheids*.

As time has gone by, more and more RR Lyrae's were observed. In the second half of the 20th century there were attempts to catalogize the RR Lyrae stars. One of these catalogues was made by Heck & Lakaye (1977) and it contained 5855 field RR Lyrae stars. About a decade later it was updated to the 6367 RR Lyrae stars (Heck, 1988). Both versions are based on the GCVS and on the general literature. Nowadays, with a help of the advanced technologies, the number of RR Lyrae's increased above a hundred thousand. For example, *Gaia* DR2 results into the 140 784 RR Lyrae stars of which about 50 220 were newly discovered (Clementini et al., 2019).

1.2 Brief characteristics

RR Lyrae stars are radially pulsating stars with periods from 0.2 to 1.2 day and amplitudes varying from 0.2 to 2.5 mag (Smith, 1995). On a Hertzsprung-Russell diagram we can find them on the horizontal branch within the instability strip (Fig. 1.1) and they belong to the spectral classes A-F. Masses of the RR Lyrae's are about 0.7 $M_\odot$ and their effective temperatures are in a range from 7400 K to 6100 K. They are giant stars with a radius interval from 4 to 6 $R_\odot$ (Smith, 1995).

With their evolution in a late stages (age typically over 9 Gyr), they are observed mostly in the globular clusters and in the Milky Way's stellar halo. They are useful in a distance measurements of the stellar systems such as above mentioned globular clusters and the elliptical galaxies, that usually does not contain classical cepheids. Based on the differences in the light curves, Bailey (1902) established three main types of RR Lyrae variables: RRa, RRb and RRc.

Later on RRa and RRb was merged into RRab because of a similarity in pulsation. The pulsation characteristics and types will be discussed in section 1.4.

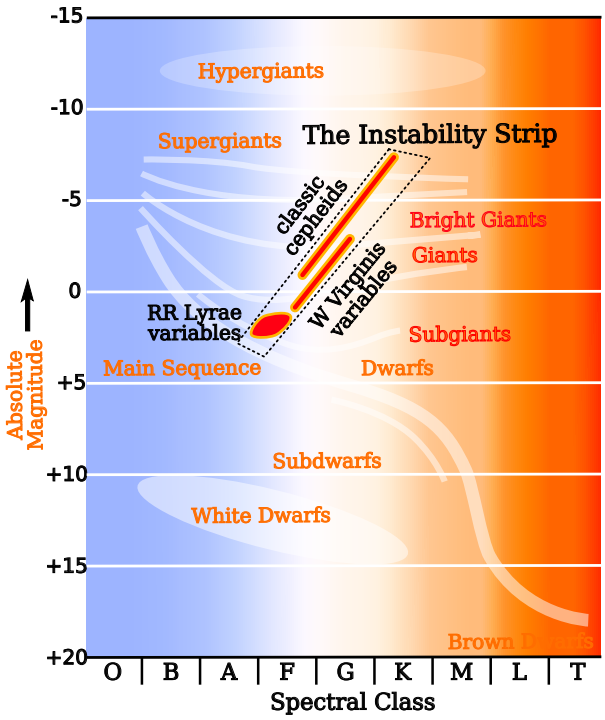

Figure 1.1: Hertzsprung-Russel diagram with the instability strip [e1]

1.3 Evolution of low-mass stars

As the low mass star begins its life on the Main Sequence, almost all radiation originates from the nuclear fusion in the core. The reaction producing this fusion is called proton-proton chain, in which hydrogen is converted to helium due to reactions between protons. Helium created by this reaction slowly builds up an inert helium core, but the core is too cool to ignite helium fusion. The Main Sequence lifetime of the low mass star (about 1 $M_{\odot}$) is approximately 10 Gyr.

With rising density, the helium core collapses and starts to heat up. Hydrogen burning zone moves into the thin shell surrounding the core and as the temperature rises, fusion became faster. More heating from the fusion results in an expansion of the star's envelope, following with cooling of the surface layers. The star gets brighter and redder and starts climbing up the Giant Branch.

Climbing the Red Giant Branch takes a star approximately 1 Gyr. During that time the helium core is contracting and heating (still without fusion). Hydrogen is burning to helium in the shell that surrounds the core and behind this shell there is huge envelope of a star. At the top of the Red Giant Branch, the core reaches temperature of 100×10^6 K. As a helium flash (short and intense explosive helium fusion) occurs, a new source of fusion ignites – the triple-alpha process. In this process the fusion of three alpha particles forms carbon nucleus.

After the helium flash, the star leaves the Giant Branch and moves onto Horizontal Branch. The location of a star in effective temperature along Horizontal Branch depends on the metallicity and on the total stellar mass whose value is related to the mass loss during the Red Giant Branch evolutionary stage (Cassisi & Pietrinferni, 2021). If the star at the Horizontal Branch passes through Instability Strip, where the hydrostatic equilibrium is disturbed, then it begins to pulsate like RR Lyrae type variable.

1.4 Radial pulsations

After the failed attempt to explain observed light variations of the Cepheid variables and cluster type variables with binary theories, Shapley (1914) suggested that the variability was caused by the pulsation. Later Eddington (1926) described an engine-like mechanism of radial pulsations, where a layer of a stellar material inside the star behaves like the valve (so-called Eddington's valve).

The working principle of the valve is as follows: During compression, the layer becomes more opaque. As the heat accumulates under the layer, the pressure starts pushing it away. After expansion the layer cools and becomes less opaque, so the radiation can easily escape and pressure drops. The cycle repeats as the layer falls back inward.

However, stellar gas usually does not behave in this way. According to Kramer's Law: $\kappa \propto \rho T^{-3.5}$, opacity κ decreases with rising temperature T. This problem was later solved by Zhevakin (1953) which identified partial ionisation zones, where energy is used to ionise the material instead of increasing heat, as a result the opacity increases. This mechanism is named after the greek letter κ for the opacity as the *κ-mechanism*.

The *κ-mechanism* is later reinforced by the *γ-mechanism*, in which the flow of heat into the cooler ionisation zone induce further ionisation. This reinforcement is caused by decrease in the ratio $\gamma = C_P/C_V$ of specific heats C_P and C_V in the layer.

In most of the stars there are two main partial ionisation zones with different positions within the star. The hydrogen partial ionisation zone is located in depths with temperature between 10 000 K and 15 000 K and is important for Mirids and ZZ Ceti variables. The helium II partial ionisation zone is located in depths with temperature of about 40 000 K and it's important for other radially pulsating stars.

For the heat engine to be effective, the location of these zones has to be in optimal depth, which is given by the star temperature. For stars with surface temperature cooler than ≈5500 K, the partial ionisation zone is too deep and the pulsation amplitude is too small. On the other side, for stars with surface temperature hotter than ≈7500 K, the partial ionisation zone is too close to surface where layers are not dense enough to absorb much energy for pulsation. These conditions determine the boundaries of the Instability Strip (Fig. 1.1).

The way in which the star pulsate is described by the radial pulsation modes. The mechanism is similar to the stationary waves inside a whistle. In the first mode (fundamental-mode) the node is in the centre of star and whole star oscillate in the same direction. The star can also oscillate in higher modes, the condition is that in the centre there is a node and the surface is oscillating. In the second mode (first-overtone mode) there is node in the centre and nodal sphere in middle parts of star – stellar material oscillate about the nodal sphere in opposite directions. The third mode (second-overtone mode) has two nodal

spheres, this divides the star into three parts – the middle one is oscillating oppositely to the other two.

1.5 RR Lyrae stars as variable stars

In order to classify variable stars, astrophysicists created the groups, classes and types based on the variability mechanisms. In Fig. 1.2 we can see the distribution of variable stars based on data taken from the latest version of the International Variable Star Index (Watson et al., 2006). Data were sorted by the variability groups found in *Variable star type designation in VSX* [e2]. The RR Lyrae are the most common regularly pulsating stars, considering their 24% fraction in pulsating stars class.

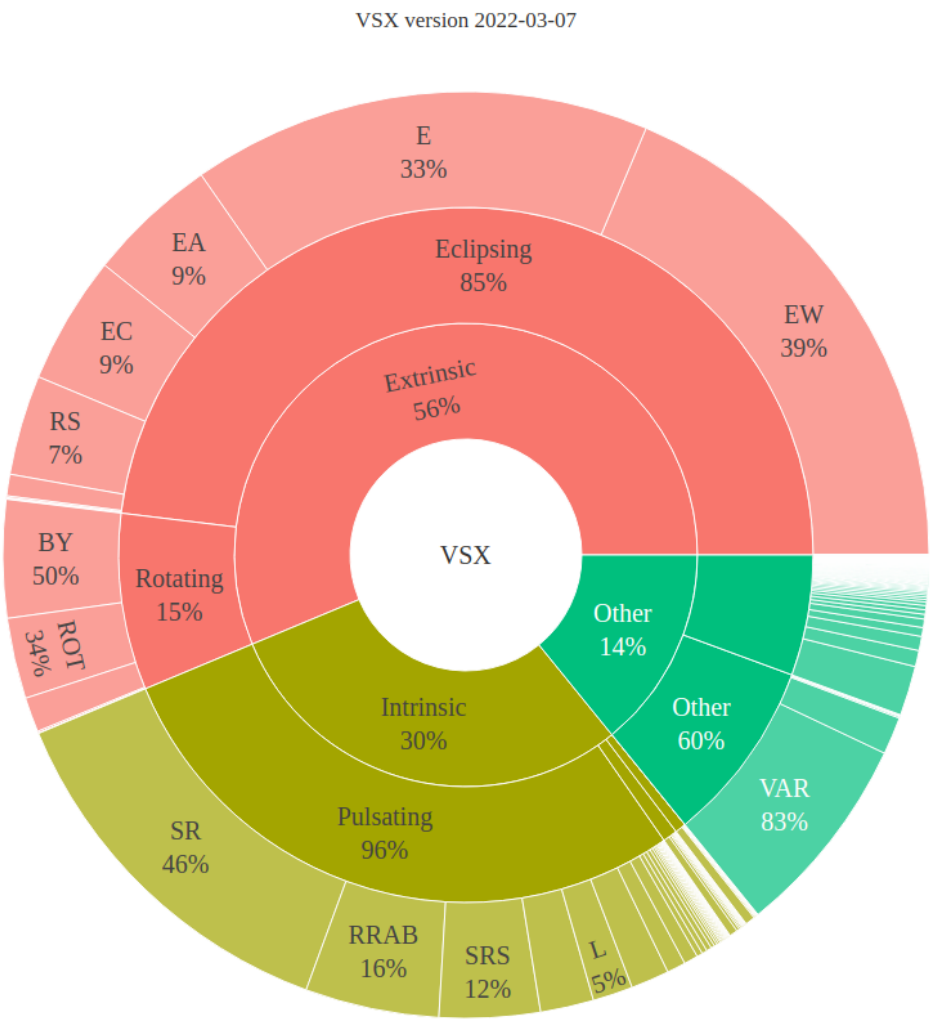

Figure 1.2: Representation of the variable stars types in the AAVSO International Variable Star Index catalogue (VSX), Version 2022-03-07.

1.5.1 Types of the RR Lyrae stars

As we mentioned in the section 1.2, the RR Lyrae stars are divided into three main types (RRa, RRb and RRc) and less common secondary types (RRd and RRe). Of which the first two were merged into type RRab due to same pulsating mode (Schwarzschild, 1940). There is also newer notation made by Alcock et al. (2000) with numerical indices based on pulsation mode: RR0 (RRab), RR1 (RRc), RR01 (RRd) and RR2 (RRe). In this thesis we will be using the original notation. The characteristics of some RR Lyrae types are as follows:

- **RRab** – As we can see in the figure 1.3, the phased light curve of the RRab type is asymmetric with steep brightening and slow fading. The RRab stars are pulsating in the fundamental mode with period in range 0.3 - 1.0 day [e3]. The fraction of the RRab type in a data shown in the figure 1.2 is about 16% of the pulsating stars.

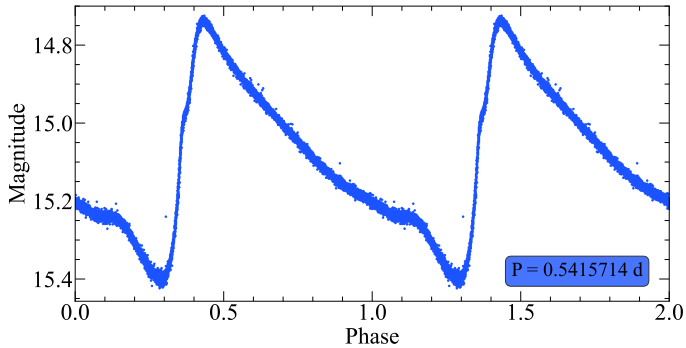

Figure 1.3: Phase curve of the RRab type star (OGLE-BLG-RRLYR-12095) – fundamental-mode pulsator.

- **RRc** – Contrary to the RRab, the phased light curves of RRc stars are symmetric with smaller amplitude (see figure 1.4). Due to the almost sinusoidal phase curve, RRc can be misidentified as other variable stars such as δ Scuti. The RRc stars are pulsating in the first-overtone mode with period range 0.2 - 0.5 days [e3]. The fraction of RRc type in data shown in figure 1.2 is about 7% of the pulsating stars.

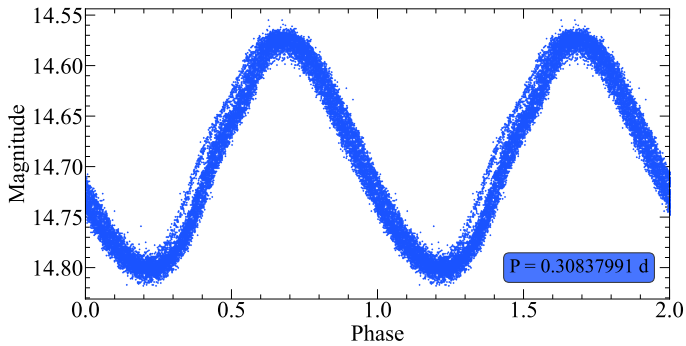

Figure 1.4: Phase curve of the RRc type star (OGLE-BLG-RRLYR-09696) – first-overtone pulsator.

- **RRd** – The RRd stars are double-mode pulsators as they pulsate in the fundamental and the first-overtone mode simultaneously. After the mode separation (see figure 1.5) we can compare individual pulsation modes with RRab and RRc. While first-overtone mode is similar to the RRc, the fundamental mode is different from RRab – it is symmetrical and the amplitude is much smaller. The RRd stars makes up approximately 0.2% of the pulsating stars in the data shown in the figure 1.2.

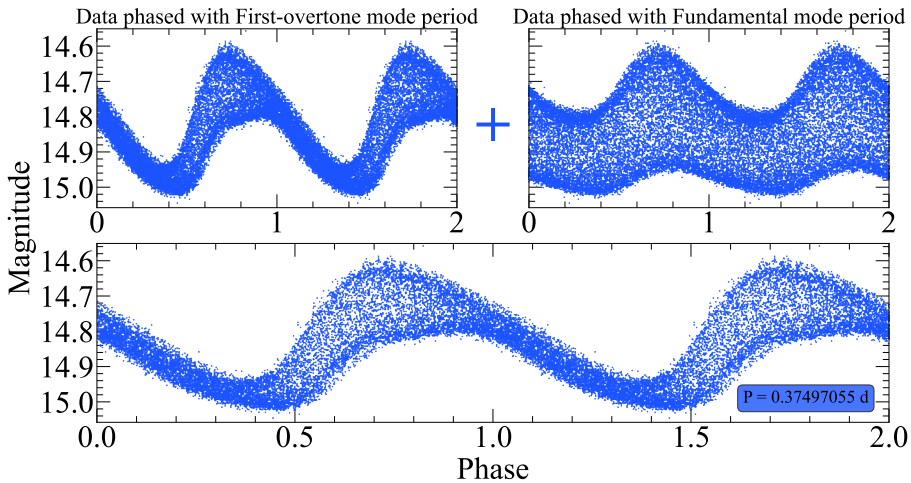

Figure 1.5: Phase curve of the RRd type star (OGLE-BLG-RRLYR-10510) – double-mode pulsator. Period of the Fundamental mode is 0.503 071 9 d and period of the First-overtone mode is 0.374 970 55 d.

The RRd stars are not the only multi-mode pulsators, in fact the RR Lyrae stars can pulsate in other combinations of radial modes. For example RR02 (fundamental and second-overtone mode) or RR012 (fundamental, first-overtone and second-overtone mode) (Moskalik, 2013; Jurcsik et al., 2015).

The Blazhko effect

2.1 Introduction to the Blazhko effect

At the beginning of the 20th century, the russian astronomer Sergei Blažko (1907) reported the periodic changes in the timing of light maximum for the RW Dra star, which was the phase modulation. Later Shapley (1916) observed the different heights of light maximum in the RR Lyrae itself, defining amplitude modulation. This phenomenon was named after S. N. Blažko, and it has been described as long-term, regular, cyclic changes in amplitude and/or phase of the light curve.

Recent findings show that the Blazhko effect manifests itself in up to 50% and more of the RRab stars (Jurcsik et al., 2009; Szabó et al., 2014; Molnár et al., 2022). The phenomenon is quite mysterious as it has not yet been sufficiently explained. Explanation is also complicated by the fact that for some stars the Blazhko effect disappeared after a while and then reappeared or within the stars where it was never observed, it suddenly appeared.

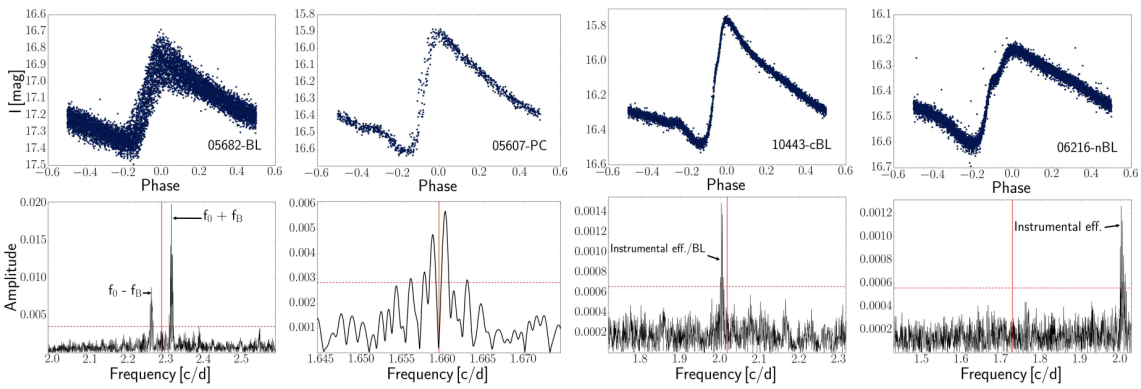

Figure 2.1: Examples of phase curves and frequency spectra of RR Lyrae stars. From left to the right: Blazhko effect, period changes, Blazhko candidate and unmodulated stars. Red dotted line show the average S/N = 3.5 limit and red line show the position of the main pulsation frequency (Prudil & Skarka, 2017).

2.2 Possible models for the Blazhko effect

- **Oblique rotator** – This model proposed by Shibahashi (2000) is based on a assumption that the magnetic axis of star with strong magnetic field is oblique to the rotation

axis. The magnetic field of star appears to vary for observer as the star rotates, causing amplitude variation. This model was ruled out by Kolláth (2018) because of failing in several attributes.

- **Turbulent modulation** – Model is based on the cyclic variation of turbulent convection in the ionization zones of the star. The principle was described by Stothers (2006) as weakening and strengthening of convection because of the quasi-periodically changing magnetic field which is generated by turbulent or rotational dynamo mechanism. The Stothers idea was tested with simplified model by Smolec et al. (2011) resulting in insufficient explanation of Blazhko effect.

- **Atmosferic shocks** – The idea is that during each pulsation cycle several strong shocks or their combination occurs. There is five shocks: s1, s2, s3, s3', s4 and their combination which is called the main shock. These shocks are produced by different mechanisms such as stopping of the hydrogen recombination (s3) or accumulation of the weak compression waves (s4) and others. Gillet (2013) suggested that the Blazhko effect originates in interaction between atmospheric effects of the first overtone shock (s3') and the main shock. This model was also ruled out by Kolláth (2018) because of a contradiction with physics of stellar pulsation.

- **F/o1 beating** – This hybrid model proposed by Bryant (2014) is based on idea of two component oscillators with close frequencies, in this case the fundamental mode and the first-overtone mode. The principle is that if the first-overtone mode is exited to large amplitude, the frequency drops to match fundamental mode frequency. The two modes then became phase locked. This model was disqualified because it was incompatible with physics of stellar pulsation (Kolláth, 2018).

- **F-NR beating** – Later Bryant (2015) modified the previous F/o1 beating model to beating with non-radial modes. The principle is the same, two oscillators (fundamental mode and non-radial modes) with close frequencies interfering together. This model is close to resonant model if the nonlinear effects are included. According to Kolláth (2018) it is questionable to reach the necessary level with modulation amplitude.

- **F-NR resonance** – The model proposed by Nowakowski & Dziembowski (2001) is based on resonant excitation of non-radial mode. Significant changes in amplitude is achieved by excitation of $m = 0$ mode. For significant changes in both amplitude and phase modulation, the excitation of $m = \pm 1$ pair is predicted. However, according to Kolláth (2018) the predictions of this model cannot be checked due to lack of nonlinear 3D models.

- **9:2 resonance** – While investigating period doubling phenomenon[1], Kolláth et al. (2011) suggested that the 9:2 resonance between the 9th overtone mode and fundamental mode might be connected not only with period doubling but also with

[1] Alternating low and high amplitude cycles in the light curve and half-integer frequencies in the frequency spectra.

Blazhko effect. Later investigation shown that this hypothesis does not contradict any of the observational facts (Kolláth, 2018).

Despite the fact, that there is yet no model which completely describes the Blazhko effect (as it is observed), the last mentioned hypothesis seems to be the most promising one.

2.3 Manifestation of the Blazhko effect in the frequency spectra

In electronics, the modulation is well known technique of changing properties of some periodic wave (carrier wave) which is used for transmitting signal. Benkő et al. (2011) modified this formalism to use it on the RR Lyrae stars with light variation as a carrier wave. There are two main types of modulation: amplitude modulation and angle modulation (composed of frequency and phase modulation). The other type is combined modulation, which uses combination of mentioned main types. Brief characteristics of various modulations are as follows:

- **Amplitude modulation AM** – With AM, the amplitude of the carrier signal is changing while frequency and phase stays constant. The equation to describe a general AM RR Lyrae light curve is given as:

$$m^*_{\mathrm{AM}}(t) = [1 + m^*_{\mathrm{m}}(t)] \left[a_0 + \sum_{j=1}^{n} a_j \sin(2\pi j f_0 t + \varphi_j) \right], \tag{2.1}$$

  where $m^*_{\mathrm{m}}(t)$ represents modulation signal, f_0 is main pulsation frequency and a_0 is non-zero constant.

- **Frequency modulation FM** – It is one of the angle modulations. In case of FM, the frequency of the carrier signal is changing. The equation to describe a general FM RR Lyrae light curve is given as:

$$m^*_{\mathrm{FM}}(t) = a_0 + \sum_{j=1}^{n} a_j \sin\{2\pi j [f_0 + m^*_{\mathrm{m}}(t)] t + \varphi_j\}, \tag{2.2}$$

  where the notation is same as in equation 2.1.

- **Phase modulation PM** – The second one of the angle modulation is PM. This modulation changes the phase angle of the carrier and keeps the amplitude and frequency unchanged. It is impossible to distinguish between PM and FM signals without any previous knowledge about them (Benkő et al., 2011). The equation for general PM RR Lyrae light curve is given as:

$$m^*_{\mathrm{PM}}(t) = a_0 + \sum_{j=1}^{n} a_j \sin[2\pi j f_0 t + m^*_{\mathrm{m}}(t) + \varphi_j], \tag{2.3}$$

  where the notation is same as in equation 2.1.

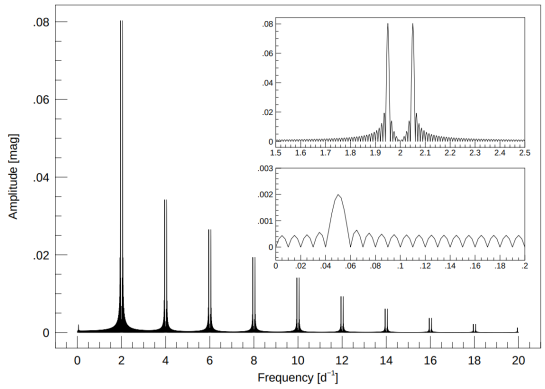

(a) Amplitude modulation. Overall spectrum (main figure), zoom around $f_0 = 2$ d^{-1} (insert top) and zoom around modulation frequency $f_m = 0.05$ d^{-1} (insert bottom).

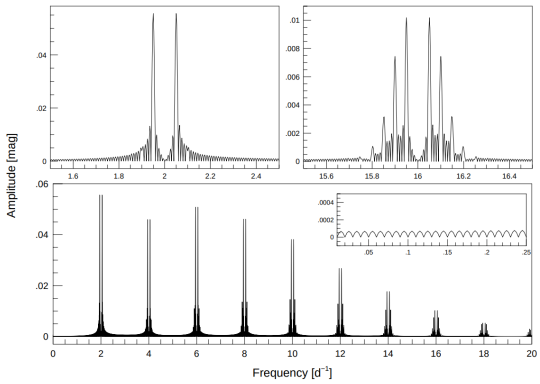

(b) Frequency modulation. Top panels: zooms around $f_0 = 2$ d^{-1} (left) and $8f_0 = 16$ d^{-1} (right), bottom: overall spectrum (main figure) and zoom around modulation frequency which is missing from the spectrum (insert).

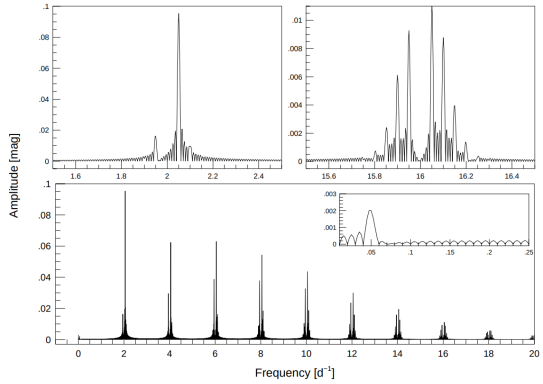

(c) Combined (AM and FM) modulation with 270° relative phase between AM and FM. Top panels: zooms around $f_0 = 2$ d^{-1} position (left) and $8f_0 = 16$ d^{-1} (right), bottom: overall spectrum and zoom around modulation frequency (insert).

Figure 2.2: Examples of Fourier amplitude spectra of an artificial sinusoidal light curves with different types of modulation. Taken from Benkő et al. (2011).

Frequency spectra of sinusoidal signal in figure 2.2 are only one of the examples. Mathematically there is no limits for complexity of modulation, therefore the modulation could be also non-sinusoidal, parallel or even cascade (modulated modulation).

The sample of stars and the datasets

3.1 Sample of stars

The RR Lyrae stars with proposed Blazhko effect was chosen from the sample of Reiner Groebel, who identified Blazhko effect from the cyclic period variations of the RR Lyrae stars. The sample consist of 142 stars. We were able to find 543 datasets for these stars in various sky surveys (Section 3.1.1). Analysis of the multiple datasets for each star should be able to confirm or deny the presence of the Blazhko effect. Identification and basic observational characteristics of the stars from our sample can be found in the appendix table 1.3.

3.1.1 Sources of the data

- **All-Sky Automated Survey for Supernovae** – ASAS-SN is survey that is observing entire visible sky every night thanks to 24 telescopes that are distributed around the world (Hawaii, Chile, Texas, South Africa and China). The focus of survey is on bright supernovae, but the data from survey are useful for research of any kind of variable objects. ASAS-SN is observing in two photometric passbands (V and g) with magnitude range from 9 to 18 (Shappee et al., 2014; Kochanek et al., 2017). Total number of datasets from ASAS-SN in our sample is 304 for 142 stars.

- **Super Wide Angle Search for Planets** – SuperWASP or SW consist of two observatories (La Palma and South Africa). This allows them to observe both North and South hemisphere. Each observatory consists of 8 wide-angle cameras that are primarily used for searching for exoplanet transit events, they are also useful for studying other variable objects. SW is able to deliver data in V passband with magnitude range from 7 to 11.5 with high accuracy and up to 15 magnitude with lower accuracy (Pollacco et al., 2006). Total number of datasets from SW in our sample is 108 for 43 stars.

- **Catalina Sky Survey** – CSS uses three telescopes, all of them are located in Santa Catalina Mountains, Arizona. The first is 1.5 m telescope with limit magnitude of 21.5 in V passband. The second one is 1 m telescope with limit magnitude of 22.0 in V passband. The last one is 0.7 m telescope with limit magnitude of 19.5 in V passband. Main mission of CSS is to locate and track near-Earth objects, but the data can be used also for other variable objects (Drake et al., 2009). Total number of datasets from CSS in our sample is 93 for 87 stars.

- **Other** – Some of the datasets in our sample came from Northern Sky Variability Survey (NSVS), which is temporal record of the sky that was conducted from New Mexico. The magnitude range of this survey is from 8 to 15.5 in the optical spectrum (Woźniak et al., 2004). Total number of datasets from NSVS in our sample is 20 for 20 stars. The last survey with 10 datasets for 10 stars in our sample is Qatar Exoplanet Survey (QES). This survey is also located in New Mexico and is using similar technology as SuperWASP (Alsubai et al., 2013).

3.2 Processing of the data

3.2.1 Primary characteristics of data

As we can see in figure 3.1, most of the stars have data in the ASAS-SN *V* filter (effective central wavelength of 551 nm, FWHM[2] of 88 nm). The second largest representation in datasets belongs to the ASAS-SN *g* filter (effective central wavelength of 480 nm, FWHM of 141 nm). Other surveys (SW, CSS, NSVS and QES) uses broad band filters in visible spectrum.

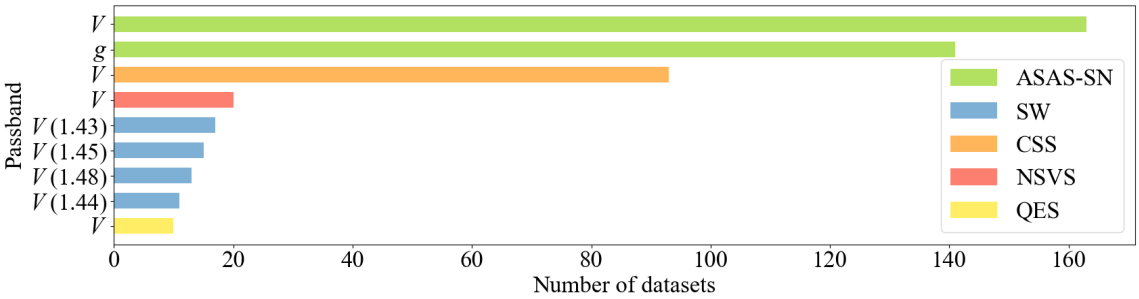

Figure 3.1: Diagram showing the number of datasets from surveys based on the passband. Passbands with less than 10 datasets are not included. In the case of SW, the filter is broad band *V* (400 - 700 nm) and numbers are camera designations.

During the inspection of datasets, we find out that some of the datasets were duplicated, these datasets were discarded from frequency spectra analysis. Remaining datasets were also checked for the range of data (time span) and number of datapoints (see figure 3.2). The cadence and the time span are important factors when searching for the Blazhko effect. These factors affect the detectability of the Blazhko peaks in spectra. Majority of datasets from the SW consists of large amount of datapoints in short time span of up to 500 days, on the other hand majority of datasets from the CSS consists of small amount of datapoints in large time span (up to 3100 days). Datasets from the ASAS-SN form two groups (see figure 3.2) – one group with small amount of datapoints (up to 1000) and small time span (up to 700 days) and the other group with larger amount of datapoints (up to 2000) and large time span (up to 2500 days). Since the Blazhko effect has large range of periods, we analyzed all of the datasets, despite of the low cadence or low observation time span in some of the datasets.

[2]Full width at half maximum.

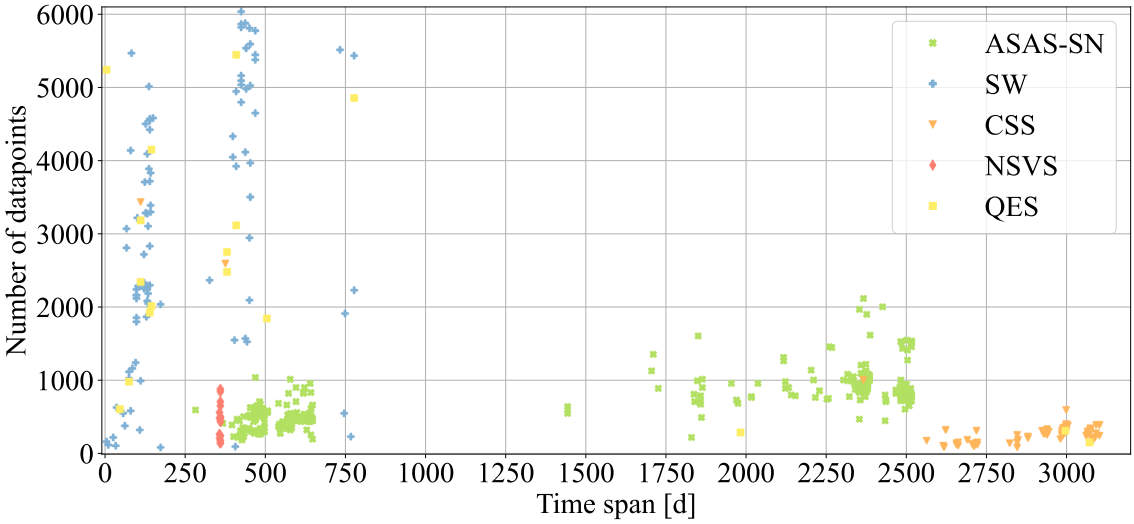

Figure 3.2: The distribution of the data sample length (the time of the last observation (HJD_F) minus the time of the first observation (HJD_I)) and number of points of each dataset. Colors and markers represents the survey from which the data was taken.

3.2.2 Software processing

- **Determination of periods with PERIOD04** – The first step in processing our data was to obtain accurate periods for each star in the sample. For this, we used PERIOD04, time string analysis software designed by Lenz & Breger (2005). In this software, we used Fourier analysis tool for initial estimation of frequencies and Fit Module tool to improve the frequencies. Mentioned procedure was made for all significant harmonics (kf_0 with k being integer number) of the basic pulsation frequency (f_0), until there was no significant peak (signal to noise ratio larger than 4) in Fourier spectra due to noise. Results of the period analysis can be seen in appendix, table 1.3 (column P_{puls}).

- **Harmonic-function fitting with LCFIT** – In the next step, we used LCFIT, which is a harmonic-function fitting program designed by Sodor (2012), to obtain frequency spectra residuals. This program uses linear and non-linear fitting as well as Levenberg-Marquardt least square fitting for parameters optimization. Initial parameters of fitting are entered in the `fitdef` file, which consist of main pulsation frequency (obtained in the first step), Fourier terms to be fitted (multiples of f_0) and epoch (the time of first datapoint of the input file). We used LCFIT due to possibility of automatize the process of obtaining residuals which is then more effective than the same process in the PERIOD04.

Analysis of the frequency spectra

4.1 Searching for the side peaks

The final step after pre-processing data, was to find presence of the Blazhko effect in RR Lyrae stars frequency spectra and to obtain Blazhko periods, i.e. identify the equidistant side peaks around f_0. For this we used `Python` script `BLSearch` (developed by Dr. Zdeněk Prudil and later modified by Dr. Marek Skarka) that allows us to visually analyse peaks around the main pulsation frequency, mark them interactively and then examine whether the Blazhko peaks are present in the spectrum around $2f_0$ (see figures 4.1, 4.2 and 4.8).

The script works semi-automatically to make it easier to analyse large amount of datasets. After we run the script (see 4.1), it gradually reads through the list of datasets parameters (which contain columns with name of dataset, epoch and the main pulsation frequency – each row represents single dataset) and loads residuals obtained with LCFIT. Then, the `matplotlib` enviroment window is open (see figure 4.1).

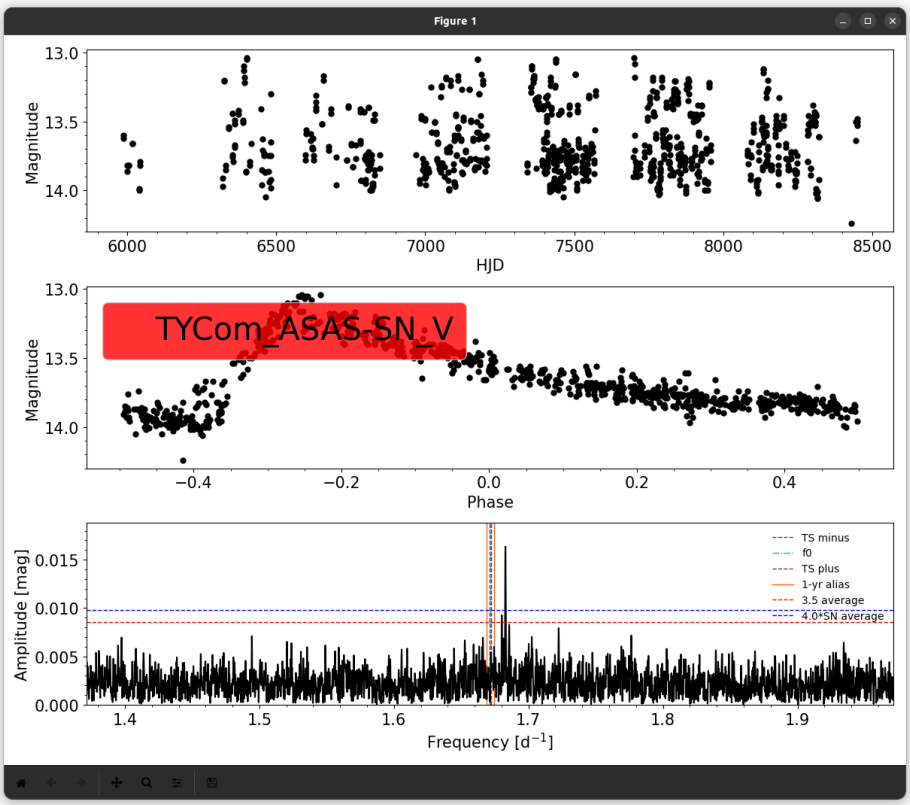

Figure 4.1: The first window that opens after running `BLSearch`.

In the top panel of figure 4.1 we can see time series of the star, middle panel shows us the data phase-folded with the pulsation period and the name of the dataset (in red rectangle) and in the bottom panel, there is frequency spectrum around the main pulsation frequency. We are able to zoom closer on the frequency spectrum and mark significant peak (see figure 4.2). After marking the peak, red square appears at the position (bottom panel of figure 4.2), the exact position of the top of the peak is found automatically, and mirrored position of this peak (solid red line) is displayed on the other side of the main pulsation frequency (see the bottom panel of figure 4.2).

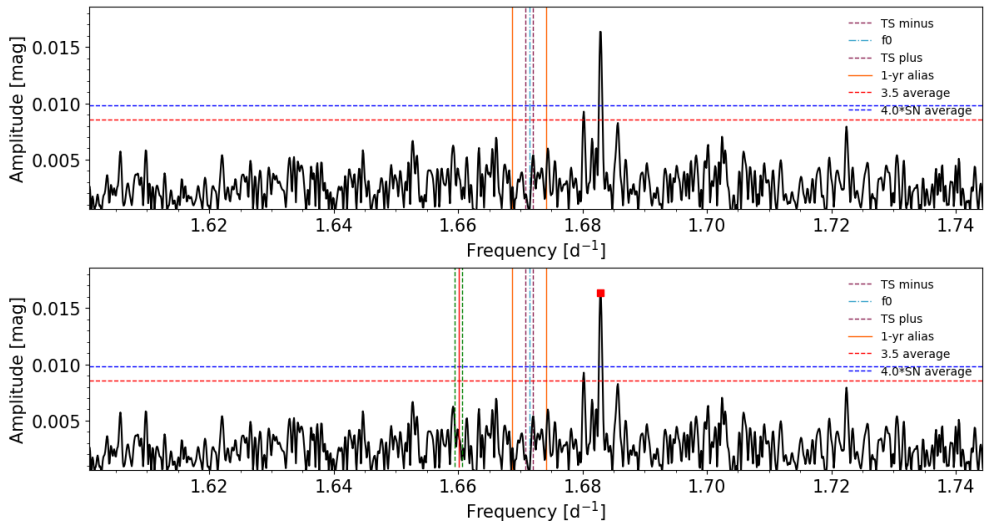

Figure 4.2: Zoomed part of the frequency spectrum (top) and the same figure with marked peak (bottom).

After we mark the peak, we can close the first window. The script then asks for the category of the star. The possible answers are:

- ***B*** – There are two optional criteria for star to be categorized as ***B***: two equidistant significant side peaks around f_0 (i.e. $f_0 \pm f_{\mathrm{m}}$) or one significant side peak near f_0 and one or more significant peaks in assumed BL positions around $2f_0$. For the examples see Figures 4.3, 4.4 and 4.5.

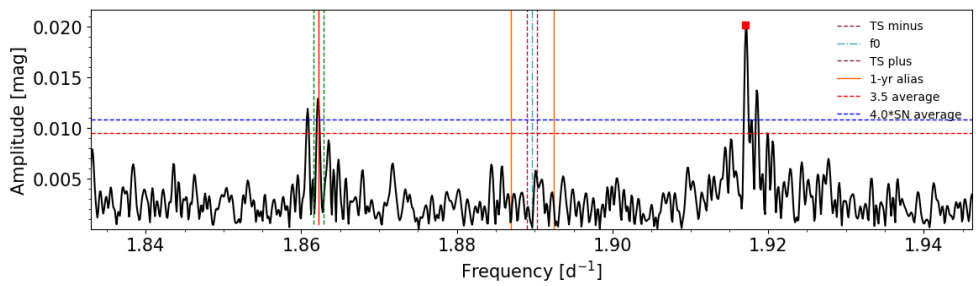

Figure 4.3: Frequency spectrum of a ***B***-category star NQ Dra (ASAS-SN *V* data) showing two significant equidistant peaks around f_0.

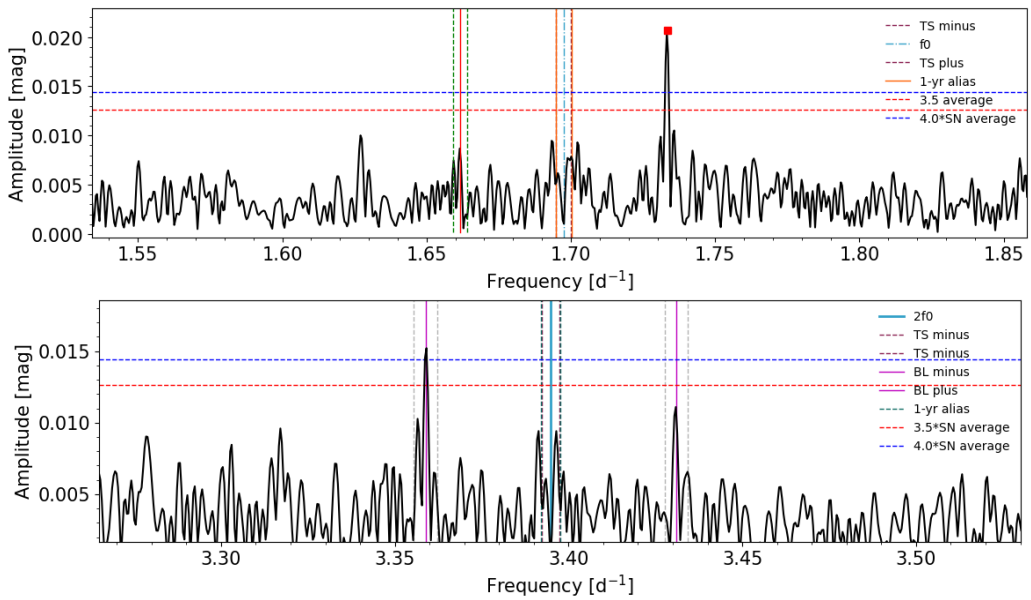

Figure 4.4: Frequency spectra of CM UMa (ASAS-SN g data) with one significant peak near f_0 (top) and one significant peak at assumed BL minus position ($2f_0 - f_m$), which make CM UMa a ***B***-category star.

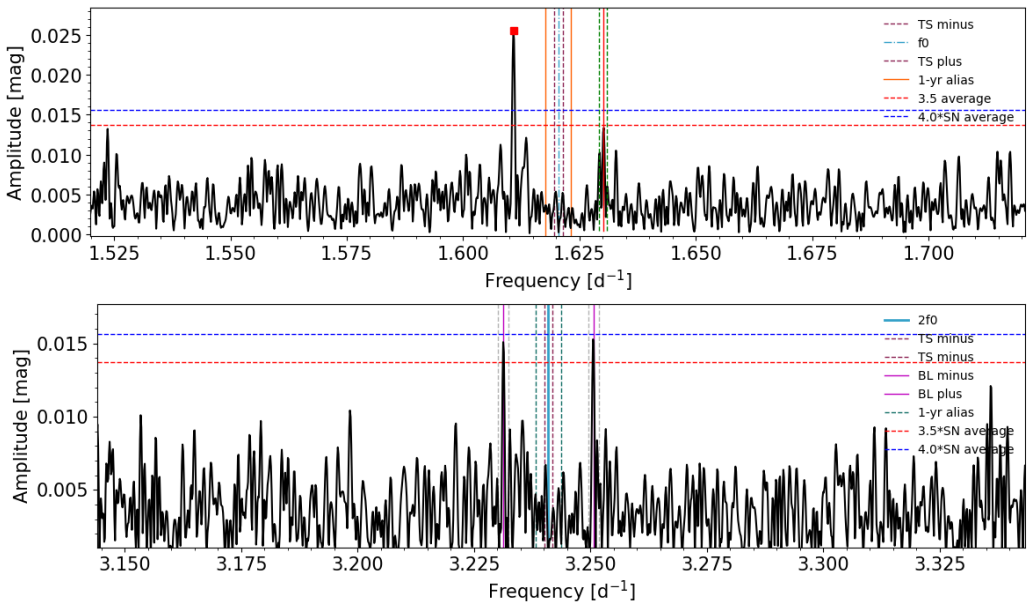

Figure 4.5: Frequency spectra of ***B***-category star KX Boo (ASAS-SN V data) with one significant peak near f_0 (top) and two significant peaks at assumed BL positions ($2f_0 \pm f_m$).

- ***BC*** – The star is identified as ***BC*** when there is only one significant peak near f_0, but no peaks in assumed BL positions around $2f_0$. An example of ***BC*** is shown in figure 4.6.

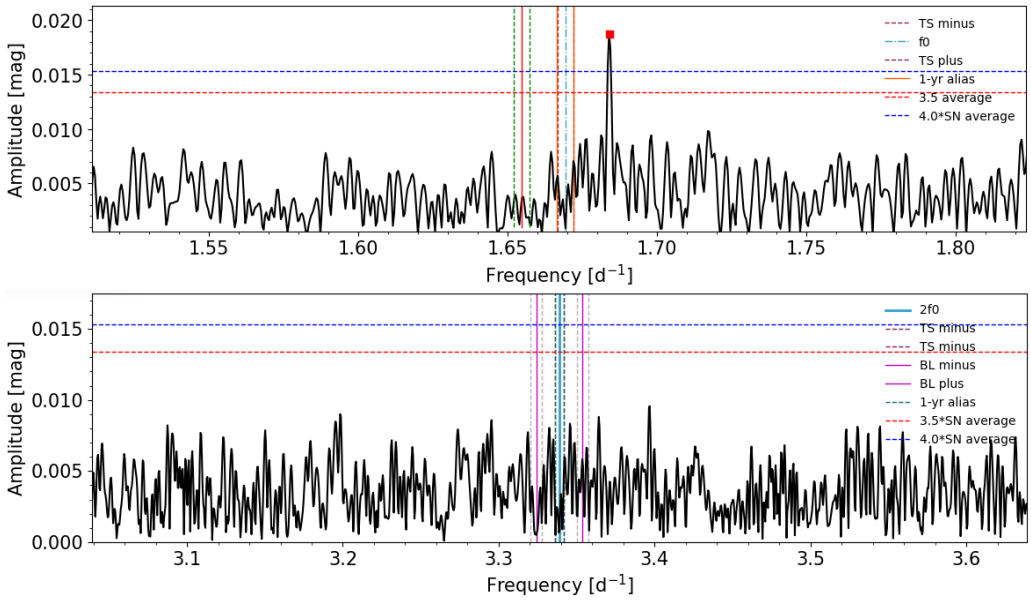

Figure 4.6: Frequency spectra of ***BC***-category star NS UMa (ASAS-SN g data) with one significant peak near f_0 (top) and no significant peak (bottom) at assumed BL positions near $2f_0$.

- ***S*** – When there is no significant peaks near f_0, the star belongs to category ***S*** (see figure 4.7).

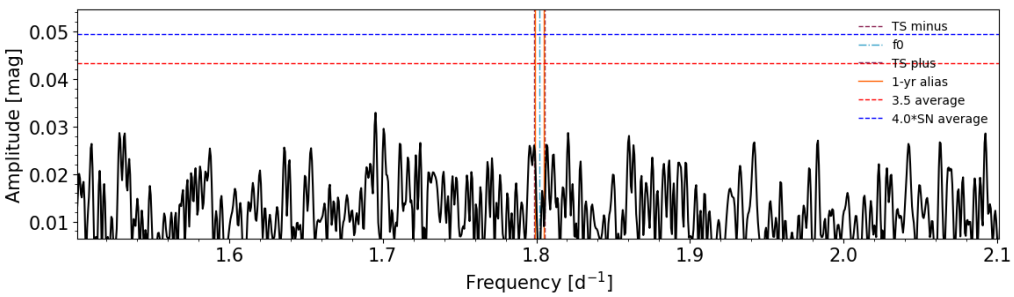

Figure 4.7: Frequency spectrum of the ***S***-category star BI Com (ASAS-SN g data) with no significant peaks around f_0.

In case of category ***S***, the script is terminated or it is continuing to the next dataset. If we select category ***B*** or ***BC***, the second window opens, in which the section of frequency spectrum around $2f_0$ is displayed (see figure 4.8). Now we can see assumed positions of the Blazhko peaks (purple solid lines) and confirm whether the Blazhko effect is present or not.

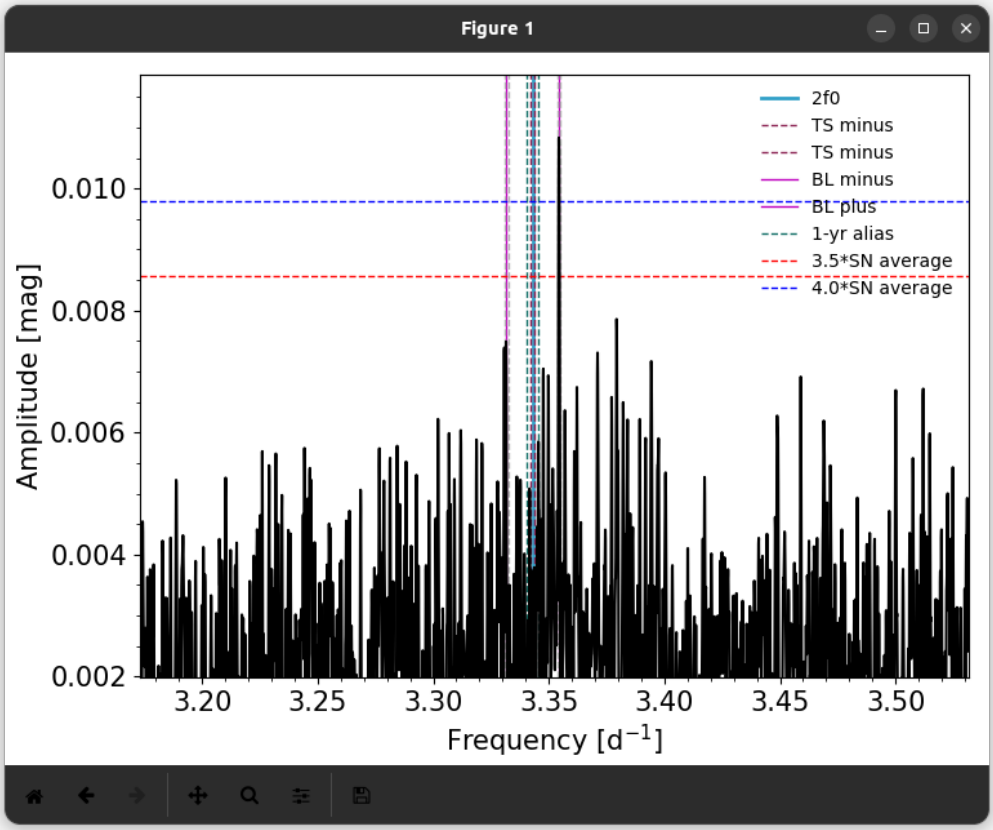

Figure 4.8: The second window of the `BLSearch`, that opens after choosing ***B*** or ***BC*** category, showing frequency spectrum around $2f_0$.

From figures 4.1 - 4.8, one may notice that there are some auxiliary lines for effective visual inspection of the spectra. Overview of this lines and their meanings are following:

- **Time span** (purple dashed lines) – TS usually represents time length of dataset (i.e. TS = $\mathrm{HJD_F} - \mathrm{HJD_I}$), but the lines noted as TS in figures 4.2 or 4.8 actually represents frequency value of 3/(2TS), that was found to be sufficient for the identification of the signal (Skarka et al., 2016). This value is related to Rayleigh criterion – limit frequency value of 2/TS. Under this limit, it is not possible to reliably identify periodic signal.

- **One-year alias** (orange solid lines or cyan dashed lines) – Since the variable stars produce continuous signal, but the observations are discrete, aliasing can occur in sampling. This creates false peaks in frequency spectra. The one-year alias arises from seasonal observations of objects. There is also diurnal alias which is related to day/night cycles and more other aliases can occur due to observation gaps.

- **Signal-to-noise ratio** (red and blue dashed lines) – S/N is a ratio of the peak amplitude and the average amplitude of the peaks around it. Generally adopted

significance level is S/N $\geq$ 4.0 (Breger et al., 1993). We adopted the S/N $\geq$ 3.5 for the peak to be considered as significant (Skarka et al., 2016).

- **Blazhko frequency** (purple solid lines) – BL plus and BL minus represents assumed position of the peaks with Blazhko modulation frequency around $2f_0$ (i.e. $2f_0 \pm f_m$).

If there is no peak in the expected position, we can close the second window and confirm the ***BC***-category. If there is a significant peak, we can mark it and the star will be automatically classified as ***B***-category. Closing window in this case will, in addition, save the row with parameters of Blazhko frequency to a data file. The example of output is shown in figure 4.9. After analysis ends, it automatically loads next dataset on the list.

```
AVDra_ASAS-SN_g 8028.6119   0.555517059 B 0.01014727 0.03147702
AVDra_SW_1.45   3886.6109   0.555517059 B 0.01001890 0.02359782
AVDra_SW_1.43   3901.6619   0.555517059 S 0.00000000 0.00000000
AVDra_ASAS-SN_V 6019.1362   0.555517059 B 0.01006815 0.02607001
AYBoo_ASAS-SN_V 5951.1771   0.614308521 B 0.00666500 0.03324573
```

Figure 4.9: Example of the script output. Each row contains name of dataset, epoch, main pulsation frequency, category, Blazhko frequency and amplitude of the Blazhko frequency (in this order).

4.2 Results of analysis

When we assume that all of the stars in our sample are (should be) modulated, we can compare the quality of datasets from different surveys based on results of analysis. As we can see in figure 4.10, the ASAS-SN survey is the only one with more ***B***-category datasets than ***S***-category datasets. Also, the QES survey together with ASAS-SN survey are the only ones that have more ***BC***-category datasets than ***S***-category datasets, but the QES survey has lower total number of datasets.

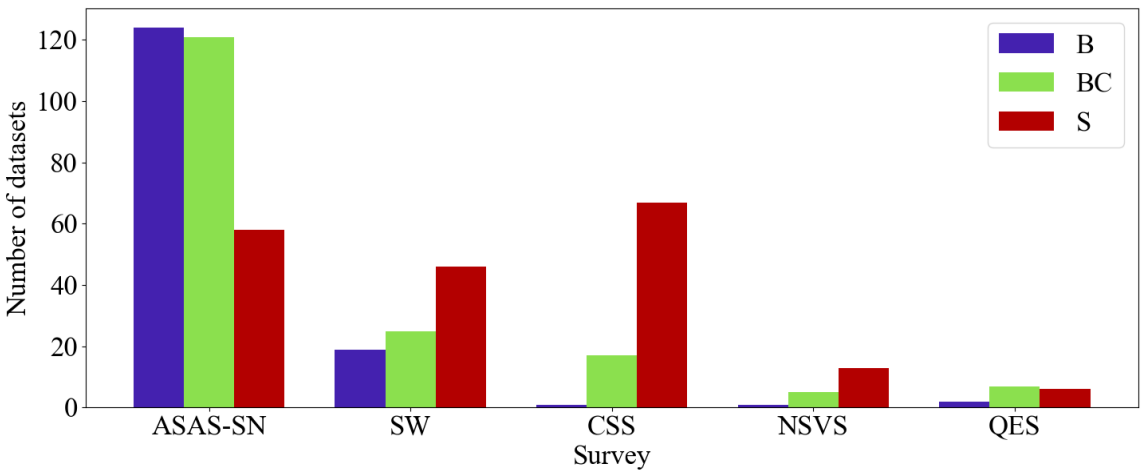

Figure 4.10: Distribution histogram of the categories (***B***, ***BC*** and ***S***) based on survey.

One of the reasons why the data from other surveys than ASAS-SN shows worse results originate in the parameters of datasets that we showed in the figure 3.2. In the figure 4.11 we display the same parameters, but with color coding based on the categories of dataset. As one may notice, all datasets with less than 1000 datapoints and less than 250 d timespan belongs to ***S***-category (mainly from SW survey). Further, most of the datasets in far right of the figure 4.11, with large time span and low number of datapoints, belong to ***S***-category (mainly from CSS survey). On the other hand, most of the ***B***-category datasets are located between 1500 d and 2500 d of the time span around 1000 datapoints line. These datasets are mainly from the ASAS-SN survey, which appeared to be the most suitable for searching for the Blazhko effect.

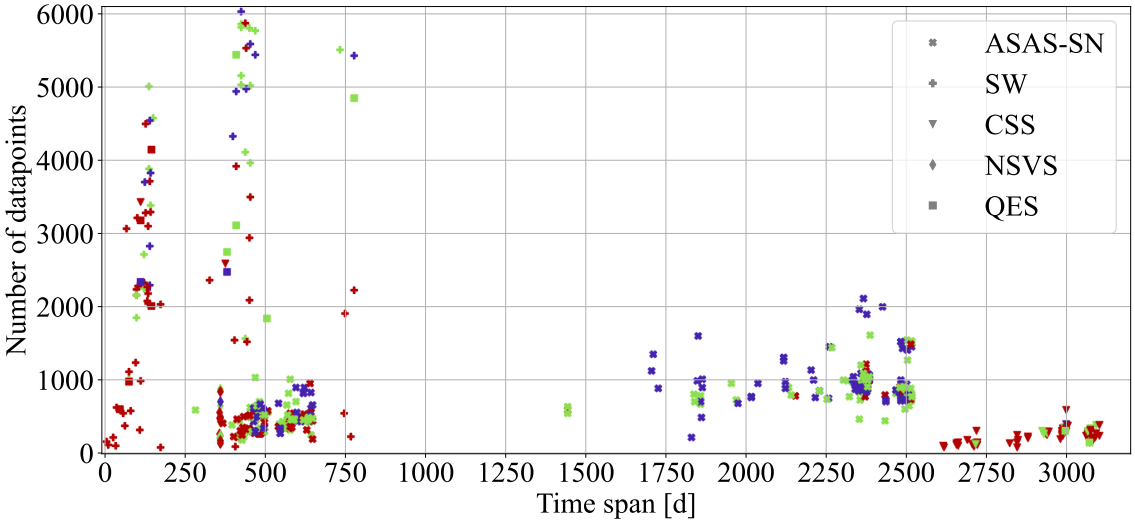

Figure 4.11: The distribution of the categories based on the timespan and the number of datapoints. Markers represents the survey from which the data was taken and colors represents identified category for each dataset (blue – ***B***, green – ***BC***, red – ***S***).

The other parameter which affects the detection of Blazhko effect in frequency spectra is the magnitude of the star, that affects the scatter of the photometric data points. In the faint stars, the modulation peaks can be hidden in noise, thus the identification of the Blazhko effect is more difficult.

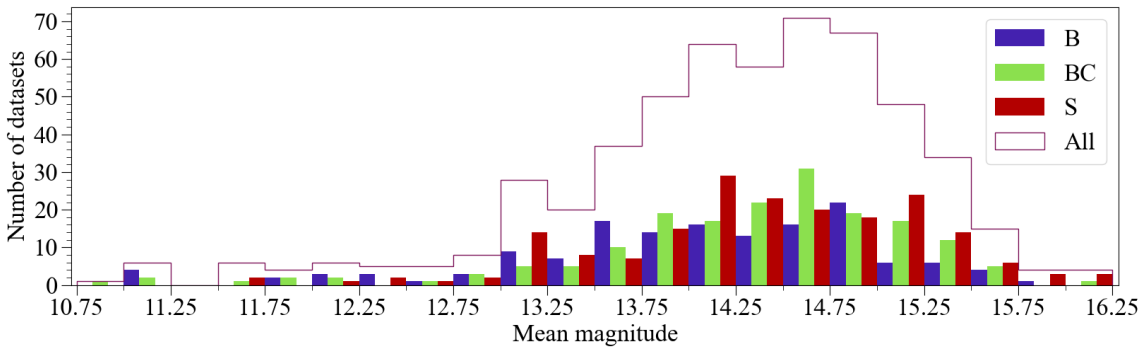

Figure 4.12: Histogram of the categories (***B***, ***BC*** and ***S***) based on the mean magnitude.

As we can see in figure 4.12, datasets with the mean magnitude over the 15 mag have significantly less detections of the Blazhko effect than the datasets with brighter stars.

4.2.1 The Blazhko periods

In the figure 4.13 we can see comparison of the period values of stars from our sample with period values of 200 stars from Blasgalf database (database of known Blazhko stars from the Galactic field, created by Skarka (2013)). Similarly to known Blazhko stars from Blasgalf, our stars shows a random distribution.

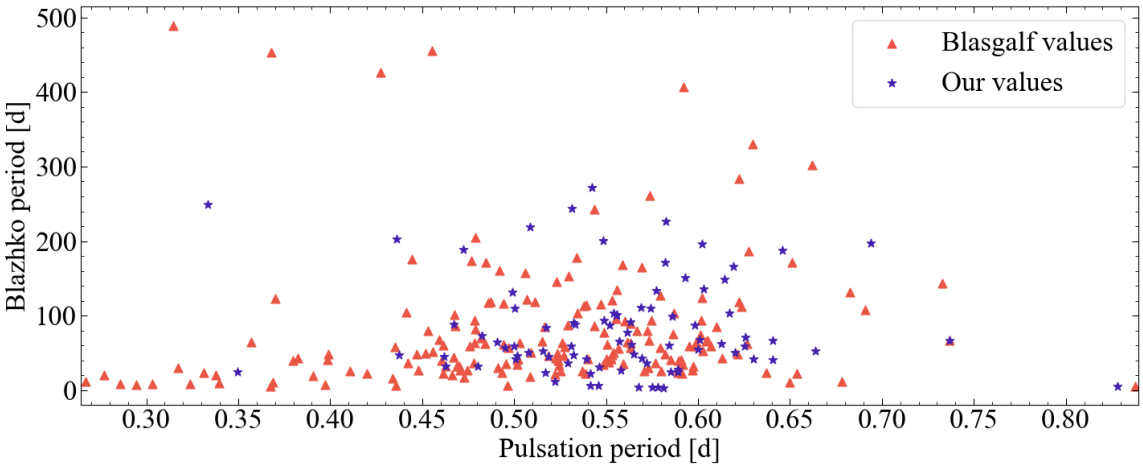

Figure 4.13: P_{BL} vs. P_{puls} diagram of RR Lyrae stars with known Blazhko effect from the Blasgalf (Skarka, 2013) and our results.

Results obtained in analysis of the frequency spectra can be seen in table 4.2, where we show 86 stars in which the Blazhko effect was identified. The second column of Table 4.2 contains Blazhko periods from works of Reiner Groebel, denoted as $P_{\mathrm{BL}}^{\mathrm{R}}$. In the third column, there are results of our analysis, specifically the mean value of the Blazhko periods obtained from different datasets. The values of Blazhko period from different datasets are shown in columns 4-8. Values that are typed with red strikethrough text are apparent outliers, that can represent some misinterpreted peak in spectra. These values were not included in the mean Blazhko period $P_{\mathrm{BL}}^{\mathrm{M}}$.

To simply evaluate our results with the results of Reiner Groebel, we created grading system with grades from 1 to 5, where the grades represent period difference between the mean Blazhko period $P_{\mathrm{BL}}^{\mathrm{M}}$ and the Blazhko period $P_{\mathrm{BL}}^{\mathrm{R}}$ determined by Reiner Groebel (see table 4.1).

Table 4.1: The grading system.

Grade:	1	2	3	4	5
Period difference [d]:	0-1	1-3	3-5	5-10	10 and more

The systematic error given by various parameters of datasets (e.g. cadence, noise, time span, magnitude of star, etc.) has larger impact on results than the measurement

error, which is highly underestimated. Due to this, we do not include error information in our results. For the example, the difference between Blazhko period obtained from the ASAS-SN *V* data and Blazhko period obtained from SW *V* data for the star NSVS 7677498 is about 2.3 d, which is much larger than usual measurement error (about 1% of measured value). Another example is CT CrB star, where the difference between ASAS-SN *V* and ASAS-SN *g* datasets is about 34 d. Because of this, we will validate our results only by the grading system.

Table 4.2: Blazhko periods of RR Lyrae stars based on the dataset with the comparison of mean periods $\left(P_{\mathrm{BL}}^{\mathrm{M}}\right)$ with periods from Reiner Groebel $\left(P_{\mathrm{BL}}^{\mathrm{R}}\right)$. The first letter of superscript at P_{BL} represents name of the survey (A for ASAS-SN, S for SW and O – as Other – for CSS,NSVS or QES) and the second letter is passband designation). In case of SW survey, two columns are displayed due to datasets from different camera.

Star	$P_{\mathrm{BL}}^{\mathrm{R}}$ [d]	$P_{\mathrm{BL}}^{\mathrm{M}}$ [d]	$P_{\mathrm{BL}}^{\mathrm{A}V}$ [d]	$P_{\mathrm{BL}}^{\mathrm{A}g}$ [d]	$P_{\mathrm{BL}}^{\mathrm{S}V}$ [d]	$P_{\mathrm{BL}}^{\mathrm{S}V}$ [d]	$P_{\mathrm{BL}}^{\mathrm{O}V}$ [d]	Grade
AV Dra	101.9	100.4	99.3	98.5	~~5.0~~	103.5	-	2
AY Boo	163	148.4	150.0	146.8	-	-	-	5
BD Dra	24.4	24.3	24.3	24.3	-	-	-	1
BF CrB	24	23.8	23.9	23.6	-	-	-	1
BH UMa	25.4	25.1	25.3	25.0	-	-	-	1
CK Com	195	197.7	197.7	-	-	-	-	2
CM UMa	27.8	27.9	27.8	27.9	-	-	-	1
CT CrB	218	219.2	201.9	236.5	-	-	-	2
CX CrB	-	4.9	4.9	-	-	-	-	-
DZ CVn	33.8	585.0	-	585.0	-	-	-	5
EM Com	279	272.0	272.0	-	-	-	-	4
ET Cep	93.8	131.4	132.9	130.0	-	-	-	5
EY UMa	94.2	93.2	93.2	-	-	-	-	1
FV Com	191	188.2	188.2	-	-	-	-	2
GU Com	65	65.1	65.1	-	-	-	-	1
IP Com	41	40.9	40.9	-	-	-	-	1
J081838.82+640526.0	59.7	59.2	59.0	59.4	-	-	-	1
J091725.57+674827.1	65.6	65.4	65.4	-	-	-	-	1
J091928.9+523123	114.2	111.4	-	111.4	-	-	-	2
J122112.22+632647.5	57.1	57.2	57.2	-	-	-	-	1
J123811.0+385027	87.6	88.8	87.6	90.0	-	-	-	2
J123844.0+651253	59.6	59.7	59.7	-	-	-	-	1
J125154.9+311814	-	6.4	6.4	-	-	-	-	-
J131756.6+375850	42.3	42.1	42.1	-	-	-	-	1
J150913.3+291713	-	4.2	4.2	-	-	-	-	-
J162435.6+584958	48.3	48.0	48.0	-	-	-	-	1
J164219.93+703750.7	27.1	27.1	27.1	-	-	-	-	1
J172906.25+644556.9	47.5	47.6	47.5	47.6	-	-	-	1
J174642.2+524530	90.3	72.8	-	-	18.5	127.1	-	5
J181425.5+561134	43	42.7	42.8	-	42.6	-	-	1
J182616.2+521011	193.9	196.1	196.1	-	-	-	-	2
J184547.86+505355.2	84.2	84.1	84.1	-	-	-	-	1
J185449.83+490305.8	36.3	37.0	37.0	-	-	-	-	1
J190603.23+742027.9	59.2	59.3	59.2	59.4	-	-	-	1
J200038.34+624146.0	24	24.7	-	24.7	-	-	-	1
KX Boo	103	103.0	103.0	-	-	-	-	1

Star	$P_{\rm BL}^{\rm R}$ [d]	$P_{\rm BL}^{\rm M}$ [d]	$P_{\rm BL}^{{\rm A}V}$ [d]	$P_{\rm BL}^{{\rm A}g}$ [d]	$P_{\rm BL}^{SV}$ [d]	$P_{\rm BL}^{SV}$ [d]	$P_{\rm BL}^{OV}$ [d]	Grade
LINEAR 12191421	134.7	133.8	133.8	-	-	-	-	1
LT Boo	453	11.4	11.4	-	-	-	-	5
LW Boo	228	91.7	4.4	179.1	-	-	-	5
NQ Dra	36.3	36.1	36.4	35.8	-	-	-	1
NSV 13707	139.6	136.0	140.2	131.8	-	-	-	3
NSV 495	46.3	46.1	46.1	-	-	-	-	1
NSVS 10592825	104.7	104.0	104.5	103.5	-	-	-	1
NSVS 2529827	240.9	244.0	244.0	-	-	-	-	3
NSVS 253439	163.3	165.8	165.8	-	-	-	-	2
NSVS 2619102	50.9	51.1	51.1	-	-	-	-	1
NSVS 2883551	56.9	55.4	55.4	-	-	-	-	2
NSVS 2896972	177	171.8	175.6	168.1	~~115.8~~	-	-	4
NSVS 2909041	66.5	66.4	66.4	-	-	-	-	1
NSVS 5033623	101.6	101.2	101.2	-	-	-	-	1
NSVS 5039297	60.4	60.5	60.5		-	-	-	1
NSVS 5302281	111.7	109.5	-	-	109.5	-	-	2
NSVS 7677498	42.4	41.7	42.5	-	40.2	42.3	-	1
NSVS 7772290	41.4	41.4	41.4	-	-	-	-	1
NSVS 7774331	223.3	226.1	224.1	228.0	144.8	-	-	2
OR Com	65	67.7	67.2	68.1	-	-	-	2
OT Dra	22.9	22.8	22.8	-	-	-	-	1
OU Dra	879	3.8	3.8	-	-	-	-	5
PP UMa	44.9	45.1	-	-	-	-	45.1	1
QQ Dra	52.9	52.7	52.7	-	-	-	-	1
TU Com	45.4	44.9	-	44.2	45.5	-	-	1
TY Com	87.5	87.1	87.7	86.6	-	-	87.2	1
TZ CVn	87	86.8	86.8	-	-	-	-	1
UW Com	89	91.0	-	91.0	-	-	-	2
UZ Com	66.3	66.4	66.4	-	-	-	-	1
V1109 Cas	187.6	203.3	203.3	-	-	-	-	5
V338 UMa	91.8	87.9	-	87.9	-	-	-	3
V343 Boo	-	248.8	248.8	-	-	-	-	-
V348 UMa	155	151.2	151.2	-	-	-	-	3
V358 Dra	77.1	77.2	77.2	-	-	-	-	1
V375 Dra	47.8	47.4	47.7	47.1	-	-	-	1
V387 Dra	-	5.8	-	-	5.6	5.9	-	-
V392 Dra	31.6	31.5	31.6	31.5	-	-	-	1
V429 Dra	111.8	99.4	-	-	-	-	99.4	5
V431 Her	-	110.3	195.4	-	25.3	-	-	-
V432 UMa	199.6	200.1	200.1	-	-	-	-	1
V464 Dra	50.2	50.2	50.2	-	-	-	-	1
V478 Dra	61.4	61.7	61.7	-	-	-	-	1
V480 Dra	60.2	62.1	62.1	-	-	-	-	2
VY CrB	32.3	32.4	32.4	-	-	-	-	1
VZ Boo	70.7	71.3	70.9	71.7	-	-	-	1
VZ UMa	-	53.0		49.8	56.2	-	-	-
WW CrB	35	3.7	3.7	-	-	-	-	5
WX CrB	32	32.4	32.3	32.5	32.3	-	-	1
WZ Com	117	188.2	187.8	188.6	-	-	-	5
XX Boo	105.6	3.5	-	-	3.5	3.5	3.5	5

From the total number of 142 stars in our sample, we identified Blazhko effect in 86 of them, which is about 60% of the sample. The results based on the grading system in the last column of table 4.2 show us that out of 86 identified Blazhko stars:

- 47 stars (55%) ended up with grade 1 (difference in range from 0 to 1 day), which we can consider as perfect match with values of Reiner Groebel. The Blazhko periods of these stars can be assumed as correct.
- 14 stars (16%) ended up with grade 2 (difference in range from 1 to 3 days), which is still considerable as a good confirmation due to systematic error.
- 6 stars (7%) ended up with grades 3 and 4 (difference in range from 3 to 10 days). The correctness of this values is questionable, but still possible to be correct.
- 12 stars (14%) got the grade 5, which is the worst grade (difference greater than 10 days). These stars needs to be closely inspected, if we want to prove the correctness of the Blazhko periods.

Lastly, 7 stars (8%) missing the information about Blazhko period from Reiner Groebel, thus we can not compare the values and grade them.

Conclusions

The purpose of our work was to analyze frequency spectra of the RR Lyrae stars obtained from the sky surveys and obtain the modulation periods, if the modulation (the Blazhko effect) was identified. For this purpose, we selected 142 stars from works of Reiner Groebel (who analyzed cyclic period variations) and got over 500 datasets to analyze. Our goal than was to confirm the Blazhko modulation and compare our findings with known Blazhko stars.

In the third chapter of the thesis, we describe the sample of stars and the datasets that we later used for analysis. The datasets that we used, come from the photometric sky surveys, particularly from the ASAS-SN, CSS, SuperWASP, CSS, NSVS and QES. Afterwards, we provided outlook on how the data was pre-processed (using PERIOD04 and LCFIT) and also on brief characteristics of our data.

The last chapter deals with the final data analysis and results interpretation. We used a custom-made interactive `Python` script `BLSearch` for the identification of the Blazhko effect and classified the stars as Blazhko modulated (***B***), Blazhko candidates (***BC***) and stable (***S***). We also displayed in-script examples of frequency spectra of stars for each category.

The main findings of this thesis can be summarized as:

- Out of 142 stars in our sample, we identified Blazhko effect in 86 of them, which is about 60% of the sample. Blazhko periods of these 86 stars were then compared with Blazhko periods from Reiner Groebel and graded. 47 stars (55%) ended up with grade 1 (difference in range from 0 to 1 day). We consider the Blazhko periods of these stars as correct. On the other hand 12 stars (14%) ended up with grade 5 (difference greater than 10 days). The Blazhko periods of these stars will need further inspection to prove them as correct.
- Out of mentioned surveys, the most suitable for searching for the Blazhko effect was the ASAS-SN survey. We identified Blazhko effect in 41% of datasets from the ASAS-SN, which is the largest percentage of detections amongst used surveys.
- We showed the importance of observational parameters (time span and cadence) on the possibility of the Blazhko effect detection. All of the datasets having less than 1000 datapoints and shorter than 250 days showed no modulation. Majority of datasets having less than 500 datapoints with the time span longer than 2500 days also showed no modulation. On the other hand, most detections of the Blazhko effect were in datasets with time span ranging from 1500 to 2500 and with about 1000 datapoints.

- We also showed the importance of star brightness, that affects the scatter of photometric points. Due to this, faint stars showed less detections of the Blazhko effect.

The results of our analysis can be seen in appendix, table 1.3, where we showing identified Blazhko periods as well as the by-product of our analysis, the improved pulsation periods of stars from our sample.

Bibliography

Alcock, C., Allsman, R., Alves, D. R., et al. 2000, ApJ, 542, 257.

Alsubai, K. A., Parley, N. R., Bramich, D. M., et al. 2013, Acta Astron., 63, 465

Bailey, S. I. & Leland, E. F. 1899, ApJ, 10, 255.

Bailey, S. I. 1902, Annals of Harvard College Observatory, 38, 1

Benkő, J. M., Szabó, R., & Paparó, M. 2011, MNRAS, 417, 974.

Blažko, S. 1907, Astronomische Nachrichten, 175, 325.

Breger, M., Stich, J., Garrido, R., et al. 1993, AAP, 271, 482

Bryant, P. H. 2014, ApJL, 783, L15.

Bryant, P. H. 2015, ApJ, 802, 52.

Cassisi, S. & Pietrinferni, A. 2021, RR Lyrae/Cepheid 2019: Frontiers of Classical Pulsators, 529, 63

Clementini, G., Ripepi, V., Molinaro, R., et al. 2019, AAP, 622, A60.

Drake, A. J., Djorgovski, S. G., Mahabal, A., et al. 2009, ApJ, 696, 870.

Eddington, A. C. 1926, The Internal Constitution of the Stars, Cambridge: Cambridge University Press, 1926. ISBN 9780521337083

Fleming, W. P. 1899, Project PHAEDRA: Preserving Harvard's Early Data and Research in Astronomy (https://library.cfa.harvard.edu/project-phaedra). Harvard College Observatory observations, 14, 815

Gillet, D. 2013, AAP, 554, A46.

Heck, A. 1988, AApS, 75, 237

Heck, A. & Lakaye, J. M. 1977, Geneva: Observatory, 1977

Jurcsik, J., Sódor, Á., Szeidl, B., et al. 2009, MNRAS, 400, 1006.

Jurcsik, J., Smitola, P., Hajdu, G., et al. 2015, ApJs, 219, 25.

Kapteyn, J. C. 1890, Astronomische Nachrichten, 125, 165.

Kochanek, C. S., Shappee, B. J., Stanek, K. Z., et al. 2017, PASP, 129, 104502.

Kolenberg, K., Smith, H. A., Gazeas, K. D., et al. 2006, AAP, 459, 577.

Kolláth, Z., Molnár, L., & Szabó, R. 2011, MNRAS, 414, 1111.

Kolláth, Z. 2018, The RR Lyrae 2017 Conference. Revival of the Classical Pulsators: from Galactic Structure to Stellar Interior Diagnostics, 6, 137

Lenz, P. & Breger, M. 2005, Communications in Asteroseismology, 146, 53.

Molnár, L., Bódi, A., Pál, A., et al. 2022, ApJs, 258, 8.

Moskalik, P. 2013, Stellar Pulsations: Impact of New Instrumentation and New Insights, 31, 103.

Nowakowski, R. M. & Dziembowski, W. A. 2001, Acta Astron., 51, 5

Pickering, E. C. & Bailey, S. I. 1895, ApJ, 2, 321.

Pollacco, D. L., Skillen, I., Collier Cameron, A., et al. 2006, PASP, 118, 1407.

Prudil, Z. & Skarka, M. 2017, MNRAS, 466, 2602.

Schwarzschild, M. 1940, Harvard College Observatory Circular, 437

Shapley, H. 1914, ApJ, 40, 448.

Shapley, H. 1916, ApJ, 43, 217.

Shappee, B. J., Prieto, J. L., Grupe, D., et al. 2014, ApJ, 788, 48.

Shibahashi, H. 2000, IAU Colloq. 176: The Impact of Large-Scale Surveys on Pulsating Star Research, 203, 299

Skarka, M. 2013, AAP, 549, A101.

Skarka, M., Liška, J., Auer, R. F., et al. 2016, AAP, 592, A144.

Smith, H. A. 1995, Cambridge Astrophysics Series, 27

Smolec, R., Moskalik, P., Kolenberg, K., et al. 2011, MNRAS, 414, 2950.

Sodor, A. 2012, Konkoly Observatory Occasional Technical Notes, 15, 1

Stothers, R. B. 2006, ApJ, 652, 643.

Szabó, R., Benkő, J. M., Paparó, M., et al. 2014, AAP, 570, A100.

Watson, C. L., Henden, A. A., & Price, A. 2006, Society for Astronomical Sciences Annual Symposium, 25, 47

Woźniak, P. R., Vestrand, W. T., Akerlof, C. W., et al. 2004, AJ, 127, 2436.

Zhevakin, S. A. 1953, Russ. Astron. J. 30, 161

Electronic sources

[e1] https://commons.wikimedia.org/wiki/File:HR-diag-instability-strip.svg (March 17, 2022)

[e2] https://www.yumpu.com/en/document/read/3589106/variable-star-type-designations-in-vsx-aavso (April 2, 2022)

[e3] http://ogle.astrouw.edu.pl/atlas/RR_Lyr.html (May 22, 2022)

Appendix

Table 1.3: List of all stars from the sample and their parameters (name, right ascension, declination, mean magnitude in V, pulsation period and mean modulation period).

Star designation	RA [hms]	DEC [dms]	m^{M} [mag]	P_{puls} [d]	$P_{\mathrm{BL}}^{\mathrm{M}}$ [d]
AP Com	12 39 18.70	+22 03 14.9	14.49	0.593607012	-
AU Boo	13 49 49.86	+16 07 47.0	15.40	0.651319326	-
AV Dra	17 59 44.21	+51 53 01.7	13.07	0.555517059	100.4
AY Boo	13 53 12.88	+17 12 45.3	14.47	0.614308521	148.4
BD Com	12 54 55.50	+23 15 25.8	14.44	0.541634478	-
BD Dra	18 17 51.94	+77 17 49.2	12.53	0.588987366	24.3
BF CrB	15 34 05.97	+33 49 47.9	14.47	0.516743248	23.8
BH UMa	10 45 55.82	+52 14 50.9	11.23	0.349361832	25.1
BI Com	13 22 44.69	+23 40 42.5	15.58	0.55495654	-
BO Boo	14 11 34.50	+31 28 18.5	15.14	0.571861584	-
BS Com	13 34 39.20	+24 16 38.0	12.76	0.363060936	-
BV CrB	16 01 27.18	+30 02 40.9	15.07	0.586753552	-
BY UMa	11 58 22.13	+55 09 41.5	15.27	0.606219119	-
CG Boo	14 16 32.21	+27 39 29.3	14.32	0.605323476	-
CK Com	12 14 50.60	+33 06 05.9	14.71	0.693965004	197.7
CL Com	12 17 16.32	+30 58 39.5	13.78	0.3604529	-
CM UMa	09 43 13.78	+49 29 37.7	13.39	0.589116062	27.9
CT CrB	16 18 34.34	+27 28 13.2	14.58	0.508594532	219.2
CX CrB	16 16 28.35	+27 52 01.4	14.08	0.828086744	4.9
DZ CVn	13 17 03.44	+36 06 58.0	14.59	0.677429976	585
EM Com	12 51 38.29	+30 31 03.4	15.39	0.542425213	272
ET Cep	01 02 23.28	+85 23 49.1	13.48	0.499036278	131.4
EW Cas	00 01 07.05	+58 33 05.9	14.25	0.540434233	-
EY UMa	09 02 20.76	+49 49 09.3	15.04	0.549052384	93.2
FL CVn	13 31 15.84	+40 56 56.8	14.66	0.514210734	-
FV Com	12 37 57.18	+29 58 05.6	14.59	0.472464103	188.2
GU Boo	15 21 54.82	+33 56 09.9	14.51	0.475072604	-
GU Com	12 39 03.27	+18 18 23.8	13.88	0.490780634	65.1
IP Boo	14 14 57.40	+39 19 23.9	14.27	0.381065137	-
IP Com	12 56 30.83	+29 53 35.8	14.89	0.640554883	40.9
J081838.82+640526.0	08 18 38.77	+64 05 26.1	15.17	0.500029223	59.2
J091725.57+674827.1	09 17 25.56	+67 48 27.1	15.15	0.557351472	65.4
J091928.9+523123	09 19 28.97	+52 31 22.3	14.58	0.568953539	111.4
J101638.51+450322.4	10 16 38.52	+45 03 22.4	15.38	0.560077768	-
J115917.3+560648	11 59 17.32	+56 06 48.6	14.74	0.533550303	-
J122112.22+632647.5	12 21 12.26	+63 26 47.8	12.96	0.495266962	57.2
J123811.0+385027	12 38 11.02	+38 50 27.0	13.64	0.533043157	88.8
J123844.0+651253	12 38 44.02	+65 12 53.6	14.22	0.531003005	59.6

Star designation	RA [hms]	DEC [dms]	m^{M} [mag]	P_{puls} [d]	$P_{\mathrm{BL}}^{\mathrm{M}}$ [d]
J125154.9+311814	12 51 54.94	+31 18 14.3	14.83	0.541367449	6.4
J131756.6+375850	13 17 56.61	+37 58 50.2	14.95	0.53932319	42.1
J141025.5+231215	14 10 25.59	+23 12 14.9	15.18	0.631283981	-
J145543.3+472759	14 55 43.32	+47 27 59.5	15.41	0.527534	-
J150913.3+291713	15 09 13.31	+29 17 13.3	15.18	0.567757029	4.2
J151404.5+330451	15 14 04.58	+33 04 51.4	15.16	0.549688014	-
J161707.8+274308	16 17 07.84	+27 43 07.0	16.22	0.612792232	-
J162435.6+584958	16 24 35.62	+58 49 58.7	14.59	0.56498214	48
J164219.93+703750.7	16 42 19.93	+70 37 50.7	14.99	0.558069971	27.1
J172135.8+374319	17 21 35.76	+37 43 19.3	13.12	0.41486301	-
J172906.25+644556.9	17 29 06.25	+64 45 56.8	15.44	0.532377902	47.6
J174642.2+524530	17 46 42.34	+52 45 30.4	14.55	0.482327684	72.8
J180624.07+522856.8	18 06 22.89	+52 28 56.0	13.57	0.586912781	-
J181425.5+561134	18 14 25.42	+56 11 35.0	14.77	0.569260558	42.7
J182616.2+521011	18 26 16.22	+52 10 11.5	14.65	0.60218831	196.1
J184547.86+505355.2	18 45 47.84	+50 53 55.0	14.78	0.517520869	84.1
J185435.96+565800.9	18 54 35.97	+56 58 00.8	15.38	0.50234074	-
J185449.83+490305.8	18 54 49.82	+49 03 05.6	14.91	0.57183602	37
J190603.23+742027.9	19 06 03.23	+74 20 27.9	13.51	0.625398433	59.3
J191617.4+725341	19 16 17.45	+72 53 41.3	13.76	0.653977254	-
J200038.34+624146.0	20 00 38.33	+62 41 45.8	15.33	0.585145821	24.7
J220219.46+630118.7	22 02 19.46	+63 01 18.7	15.42	0.539314582	-
J221333.36+652720.1	22 13 33.35	+65 27 20.1	15.44	0.429914677	-
J235643.15+490916.7	23 56 43.17	+49 09 16.7	15.33	0.51186446	-
KQ UMa	09 17 20.21	+68 38 06.0	14.46	0.486392478	-
KU Boo	14 30 30.82	+50 20 22.3	13.41	0.570641518	-
KX Boo	14 31 00.90	+20 25 31.9	14.15	0.617107173	103
LINEAR	-	-	14.88	0.279680497	-
Linear 12191421	14 34 46.09	+32 23 34.3	15.38	0.577234733	133.8
Linear 17914937	16 16 40.10	+27 46 25.0	14.08	0.414302919	-
Linear 20441941	17 12 10.88	+57 13 45.0	15.1	0.68877469	-
Linear 20801695	17 33 31.22	+61 16 08.8	14.03	0.60105734	-
Linear 5168861	08 44 28.72	+61 24 43.3	15.37	0.597438744	-
LN Boo	14 37 09.04	+25 44 46.6	13.66	0.466731987	-
LT Boo	14 38 45.15	+53 46 58.6	14.42	0.522264065	11.4
LV Boo	14 39 02.20	+53 57 44.2	14.59	0.516191741	-
LW Boo	14 40 32.61	+17 35 57.3	13.24	0.563430897	91.7
MU Boo	14 48 14.73	+19 20 19.1	13.95	0.320374699	-
NQ Dra	18 44 13.20	+57 41 00.7	13.72	0.529195514	36.1
NS UMa	08 24 24.73	+65 43 03.4	10.97	0.598998643	-
NSV 13707	21 25 29.28	+60 51 46.3	15.55	0.602869704	136
NSV 495	01 24 57.04	+52 02 40.3	12.79	0.5017709	46.1
NSV 6808	14 47 40.28	+25 58 39.1	14.86	0.5617599	-
NSVS 10592825	15 17 29.33	+22 44 39.7	14.29	0.554178516	104
NSVS 2529827	09 57 42.97	+54 06 07.5	14.54	0.531263474	244
NSVS 253439	00 28 44.88	+80 02 02.4	13.88	0.619190528	165.8
NSVS 2556476	10 20 02.85	+61 15 38.5	14.37	0.64285886	-
NSVS 2606910	11 39 58.04	+55 00 48.5	14.73	0.686432881	-
NSVS 2619102	11 24 39.70	+66 33 04.9	14.06	0.507897569	51.1
NSVS 2622540	11 34 36.24	+60 18 20.5	14.48	0.600982609	-
NSVS 2883551	17 09 46.08	+64 46 21.4	13.93	0.600181645	55.4
NSVS 2896972	16 47 08.84	+56 13 03.1	14.03	0.582020264	171.8

Star designation	RA [hms]	DEC [dms]	m^{M} [mag]	P_{puls} [d]	$P_{\mathrm{BL}}^{\mathrm{M}}$ [d]
NSVS 2909041	17 15 59.56	+54 28 10.3	13.67	0.64077841	66.4
NSVS 2932464	18 02 12.25	+56 13 59.1	14.68	0.575991378	-
NSVS 5033623	12 47 55.95	+40 25 35.1	14.83	0.555952332	101.2
NSVS 5039297	13 03 50.74	+40 21 47.6	13.55	0.584109955	60.5
NSVS 5302281	17 06 56.97	+50 20 53.7	14.32	0.574383356	109.5
NSVS 7677498	13 31 54.00	+30 00 10.9	14.69	0.500977443	41.7
NSVS 7772290	14 59 13.90	+37 02 34.1	14.74	0.63019806	41.4
NSVS 7774331	15 04 30.94	+31 38 53.7	13.91	0.582366921	226.1
OR Com	13 19 54.50	+19 53 56.8	13.34	0.600989679	67.7
OS Dra	12 12 30.37	+65 30 23.0	13.02	0.349054349	-
OT Dra	12 25 04.51	+66 38 39.7	13.83	0.541234939	22.8
OU Dra	12 47 19.46	+69 05 53.9	13.66	0.57520206	-
PP UMa	08 52 15.07	+70 26 23.9	13.69	0.518734779	45.1
PQ UMa	08 55 39.57	+60 29 36.4	13.85	0.474149286	-
QQ Dra	09 29 09.71	+48 19 04.5	13.52	0.663675405	52.7
QY UMa	09 49 54.92	+51 44 22.5	13.15	0.572022596	-
TU Com	12 13 46.95	+30 59 07.6	13.97	0.461888967	44.9
TY Com	12 22 21.36	+16 17 33.8	13.66	0.598276008	87.1
TZ CVn	13 01 29.18	+32 05 13.3	14.19	0.55188027	86.8
UW Com	12 59 52.27	+30 14 31.9	14.24	0.532306495	91
UZ Com	13 12 26.75	+30 21 16.0	13.24	0.736963233	66.4
V1041 Cas	00 32 54.17	+47 08 49.2	12.92	0.56727965	-
V1109 Cas	01 26 22.16	+73 13 11.3	13.28	0.436201552	203.3
V338 UMa	10 26 37.28	+43 34 32.2	13.83	0.467122433	87.9
V343 Boo	14 03 31.37	+08 30 43.4	14.14	0.3333505	248.8
V346 Dra	16 08 21.23	+62 29 54.5	14.17	0.534529651	-
V348 UMa	11 53 59.31	+55 14 35.5	13.44	0.592998874	151.2
V358 Dra	16 57 01.85	+66 35 11.1	14.17	0.561618387	77.2
V375 Dra	17 32 23.75	+51 40 47.3	13.09	0.43759313	47.4
V387 Dra	17 54 12.92	+51 01 22.4	12.41	0.545768485	5.8
V392 Dra	17 59 46.32	+77 41 46.1	13.81	0.546177007	31.5
V429 Dra	19 59 32.16	+61 31 21.1	15.21	0.585978533	99.4
V431 Her	17 38 32.79	+24 37 24.3	14.71	0.500436121	110.3
V432 UMa	08 53 37.75	+49 09 03.4	12.17	0.548540129	200.1
V464 Dra	14 28 55.07	+57 30 23.9	14.25	0.620092205	50.2
V478 Dra	16 03 46.99	+57 41 47.8	13.52	0.563743489	61.7
V480 Dra	16 07 37.40	+57 32 08.5	14.06	0.612696241	62.1
V506 Her	17 38 11.31	+18 53 17.2	14.17	0.607909261	-
V568 Cas	01 17 13.51	+74 51 19.8	12.62	0.514039377	-
V845 Cas	23 26 15.04	+57 23 55.4	14.52	0.570845703	-
V857 Cep	00 09 39.77	+53 10 11.0	13.88	0.56997543	-
VY Crb	16 06 11.55	+33 22 15.5	14.31	0.462952579	32.4
VZ Boo	14 53 15.89	+25 57 19.5	15.32	0.625701325	71.3
VZ UMa	11 17 28.28	+29 40 30.1	14.18	0.515513677	53
WW CrB	16 16 59.60	+39 38 36.8	14.95	0.578174402	3.7
WW CVn	13 34 30.92	+29 18 15.3	14.96	0.523369205	-
WX CrB	16 19 14.10	+39 30 08.6	13.74	0.480115277	32.4
WZ Boo	15 02 09.33	+24 29 42.2	14.01	0.577496809	-
WZ Com	12 07 34.00	+20 06 09.5	15.13	0.646003666	188.2
XX Boo	14 51 37.56	+29 21 26.7	11.87	0.581400348	3.5
YY CVn	13 55 17.18	+29 41 32.4	15.58	0.562816267	-